CRYSTALLIZATION AND THERMODYNAMIC PROPERTIES OF TITANIUM STANNIDES

O. V. Pondarevskaya[1], O. P. Petrenko[1], V. S. Sudavtzova[2], V. V. Lisnyak[2]* and N. V. Stus[2]

[1]Ukrainian State University of food technologies, 68, Volodymyrska str., 01033, Kyiv, Ukraine
[2]Taras Shevtchenko University, 64, Volodymyrska str., 01033, Kyiv, Ukraine

Abstract

Thermodynamic properties of pure titanium stannides obtained by crucible-less growth techniques under vacuum are determined by differential scanning calorimetry and Knudsen effusion. The enthalpy, specific heat capacity, entropy and Gibbs energy temperature dependence were simulated using Maier and Kelly equations. Standard enthalpies of evaporation, formation and atomization of titanium stannides were determined and compared with earlier-known data.

Introduction

The thermodynamics (TD) study of pure intermetallic compounds is of special interest for practical usage in metallurgy. The first necessary step of such study deals with single crystal growth. Absence of specific information on the pure stannides synthesis in binary system Ti–Sn, in particular, intermetallic compounds solidification mode, facilitate growth processes and alloy compositions optimization. Moreover, the extreme reactivity of the melts with oxygen and, practically, all known crucible materials require crucible-less growth techniques under high-purity inert atmosphere. Selective evaporation of alloy components and peritectic solidification mode of some compounds additionally aggravates the crystal growth process.

We synthesized Ti_3Sn, Ti_2Sn, Ti_5Sn_3 and Ti_6Sn_5 by a vertical floating zone melting technique with radio frequency (r.f.) heating for consequent thermodynamics study. Relevant parts of binary phase diagram have been determined in order to optimize the growth conditions [1].

---

*   Author for correspondence: Fax: +380-44-2712194; E-mail: lisnyak@chem.univ.kiev.ua

Experimental procedures

Phase equilibrium Ti–Sn has been studied in several issues [2, 3] by DTA, powder X-ray crystallography and electron probe microanalysis (EPMA).

Four different types of intermetallics are formed in binary Ti–Sn system. The section of the Sn–Ti phase diagram, which is relevant for the crystallization is shown in Fig. 1. Titanium stannides Ti_3Sn, Ti_6Sn_5 melt congruently at 1936 and 1667 K, respectively. Intermetallic compound Ti_2Sn, Ti_5Sn_3 were synthesized by perictectic reaction at 1825 and 1778 K, correspondingly, Ti_3Sn was crystallized in narrow homogenous area, which lies in concentration diagram section exceeded by tin.
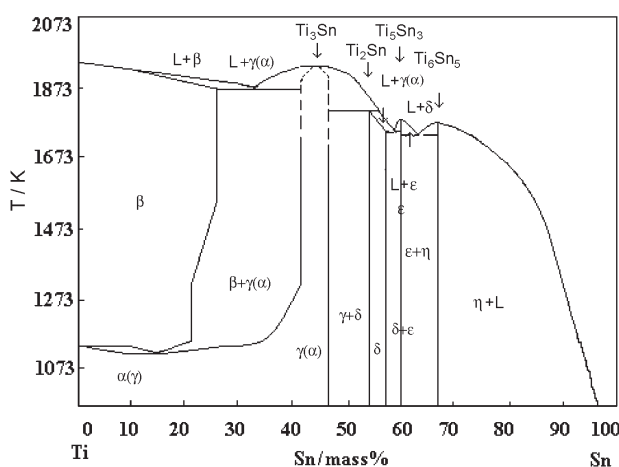

Fig. 1 Phase equilibrium in Ti–Sn system at temperature range 1073–2073 K

At first traditional arc-melting technique was used for stannides synthesis as discussed below. The polycrystalline master alloys were prepared from a mixture of the high purity (Aldrich grade) element powders with a nominal Ti:Sn ratios of 3:1, 2:1, 5:3, 6:5, which were cold-pressed into tablets and melted by arc-melting on the water-cooled copper hearth under an inert argon atmosphere. The purity of the starting materials was better than 99.99% and average particle size of the powders was less than 100 μm (to ensure a high homogeneity and remove internal stress the samples were remelted several times). Rapid cooling and homogenization procedure in solid lead to formation of polyphase material with a grain size less than 150 μm. Obtained polyphase materials (Ti_3Sn, Ti_2Sn, Ti_5Sn_3, Ti_6Sn_5 with tin and titanium polymorphs admixtures) are useless for thermodynamic study that is why a new method of pure stannides single crystals growth was elaborated.

The stoichiometry control of the master alloys is one of the key problems for the crystal preparation. The soft melting process usually minimizes selective element evaporation. For the preparation of intermetallides bulk titanium element and powder blend of Sn were pressed to pellets and melted in r.f. Hukin type cold copper crucible.

The buttons were several times remelted in an arc furnace for homogenisation and finally cast into feed rods of 6 mm diameter from the levitated melts in the Hukin type crucible. The overall mass loss was kept below 0.5%. The polycrystalline feed rods have been homogenized by annealing in vacuum up to 1673 K. The alloy was homogenized by remelting due to interaction of titanium as well as stannides (Ti_3Sn, Ti_2Sn, Ti_5Sn_3) with molten tin constituent. This procedure permits to complete the reaction of high-melting binary stannides formation at moderate temperature.

Bulk crystals were grown by a computer-aided floating zone facility with r.f. induction heating (250 kHz, 30 kW). Asymmetric counter-rotation of crystal (10 rpm) and feed rod (20–40 rpm) was employed. Growth parameters like zone travelling rate, zone temperature, radio frequency and input power were tracked during the growth process. Other parameters and features of the growth process, which are specific for a class of intermetallic compounds, are discussed in [1]. Titanium and tin content, microstructure and crystal perfection of the samples were investigated by chemical analysis, optical metallography, electron probe microanalysis (EPMA), resulted that obtained materials tin and titanium content is equal to the theoretically predicted amounts in compounds (deviation less than 0.2%).

X-ray powder study indicated that all obtained specimens are in single phase and their crystallographic parameters are identical to that for Ti_3Sn, Ti_2Sn, Ti_5Sn_3, Ti_6Sn_5 [2]. Diffraction data were collected using DRON-3 (CuK_α radiation) diffractometer.

The pure stannides single crystals: Ti_3Sn, Ti_2Sn, Ti_5Sn_3 and Ti_6Sn_5 were used for thermodynamics study. The standard enthalpies of formation, specific heat capacity and enthalpy dependence *vs.* temperature for stannides were measured on Calvet type differential automatic calorimeter (DAC-1-M). Evaporation rates of stannides were determined by Knudsen effusion using self-made vacuum evaporator.

The total vapour pressure above titanium stannides was calculated using evaporation rates data by well-known Hertz–Knudsen effusion equation modified by Clausing [4]. The effusate was analyzed by chemical analysis also by X-ray diffraction and was found to be a pure tin.

The self-made high-temperature vacuum evaporator is similar in general to instrument described elsewhere [5]. Major modifications introduced concerned with replacement of some components of electronic equipment that improved temperature stabilization of the core and balance regulation system, which made the data acquisition more versatile. As the particulars of our high-temperature instrument have not been disclosed in English language publications before, we shall briefly discuss here the general principles adopted at the design stage and highlight a few distinctive features.

The high-temperature vacuum evaporator consist of three blocks (a) the vacuum system, (b) the furnace with temperature stabilization system, (c) the microanalytical balance with data acquisition system. A scheme of the central part of instrument is shown in Fig. 2. I. It consists of two equal by volume cylindrical vacuum chambers. The microanalytical balance is located in the top chamber, while the high-temperature furnace is placed in the bottom chamber. The bottom chamber casing, top and bottom flanges are cooled by flowing water. The heating chamber contains water cooled copper electrodes (14), molybdenum cylindrical resistance heater (9) (inside

diameter 40 mm, height 150 mm, maximal furnace using power 6 kW) and W–Re 5/20 thermocouples placed in isothermal zone of the heater, nearby the effusion cell containing measured sample (10). Used graphite (Fig. 2. II,2) Knudsen cell was covered by 0.005 inch tantalum sheet (Fig. 2. II,1) with orifice, which geometry were previously measured with traveling microscope. The diameter of the cell was 0.0658±0.0009 cm and the edge of hole was 0.025±0.001 cm thick. In calculation proceeding the rate of evaporation, the orifice dimensions are corrected for thermal expansion [6].

Several vertical and horizontal reflecting shields made of molybdenum and nickel foils are placed around the heater to decrease the heat loss (7, 8, 17). The temperature inside the heater is maintained constant ±1 K by means of an analogue PID-regulator that governs the voltage supply to the lowering transformer through a bridge of electronic valves. A thermocouple (11) located in the immediate vicinity of the heater surface, in its uniform temperature zone, serves as a feedback detector of temperature. All thermocouples employed in the furnace core were made of the same consignment of thermocouple wire that had been calibrated by comparison with the exemplary Pt–PtRh/10 thermocouple. Control thermocouple was placed previously
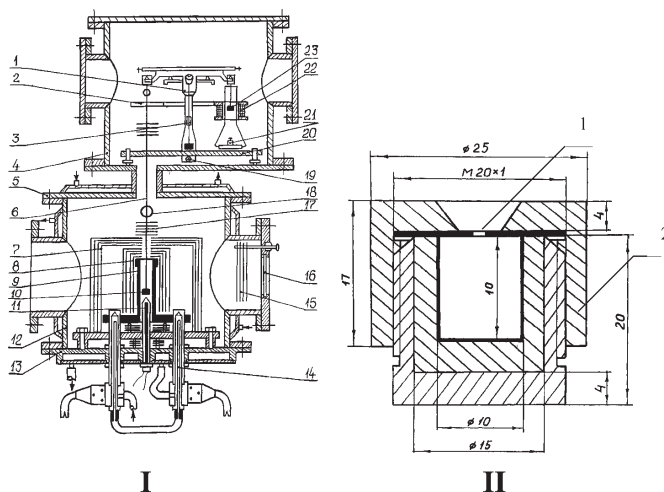

Fig. 2 A scheme of the central part of the evaporator device. See text for details
I. Scheme of evaporator device
1 – microanalytical balance BlM-20 g-M placed in vacuum chamber; 2 – ebonite balance's frame; 3 – balance dempfer; 4, 12 – top and bottom chamber casing; 5, 13 – top and bottom water cooling flange; 6 – chain; 7 – nickel and 8 – 17-molybdenum horizontal and vertical shields; 9 – molybdenum cylindrical heater; 10 – effusion cell with specimen; 11 – measured and regulated by temperature regulator WRT-3 thermopiles (W-Re 5/20 type) placed in alumna cover; 14 – water cooling copper electrodes; 15 – diaphragm; 16 – looking windows; 18 – ring; 19 – arretire with low; 20 – balance body; 21 – balance scale; 22 – inductive coil; 23 – ferrit magnet's core
II. Projection view of effusion cell
1 – tantalum sheet with orifice; 2 – graphite effusion cell chamber

inside the mullite tube in the position normally occupied by the Knudsen cell for temperature correction during study. The overall accuracy of the temperature measurement is estimated to be within 1.6 K.
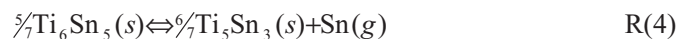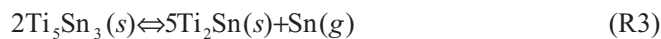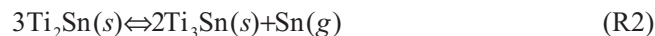
High vacuum in the evaporator system was generated by Fisher Maxima C corrosion resistant vacuum pump D2A and measured by Fisher digital pressure gauge equipped with Pirani gauge heads. At 2000 K the pressure in system during experiment was not lower than $3 \cdot 10^{-3}$ Pa.

The microanalytical balance is fixed by ebonite balance frame in the top vacuum chamber center, nickel and molybdenum shields are used for heat irradiation reflection. The microbalance is equipped with devices for fixing and removing misbalance of mass loss. The misbalance removing, measuring and correction system is principally based on controlled by IBM PC electrical scheme, which regulates ferrite magnet induction proportionally to mass losses. High purity metals (99.99% Ag, Ti, Sn) were used for microbalance calibration. The sensitivity of the balance was found to be 2.01 µg/0.001 cm, while the readings of the traveling microscopy were reproducible to 0.00025 cm. Construction of microanalytical balance in conjunction with a specific design of misbalance detector allows an increase in the sensitivity of the instrument by an order of magnitude compared with our previous model [7].

Results and discussion

Evaporation rate and total vapour pressure

Heating of stannides in vacuum lead to dissociation of compound, which is represented by chemical reactions:

$$\text{Ti}_3\text{Sn}(s) \Leftrightarrow 3\text{Ti}(s) + \text{Sn}(g) \tag{R1}$$

$$3\text{Ti}_2\text{Sn}(s) \Leftrightarrow 2\text{Ti}_3\text{Sn}(s) + \text{Sn}(g) \tag{R2}$$

$$2\text{Ti}_5\text{Sn}_3(s) \Leftrightarrow 5\text{Ti}_2\text{Sn}(s) + \text{Sn}(g) \tag{R3}$$

$$\tfrac{5}{7}\text{Ti}_6\text{Sn}_5(s) \Leftrightarrow \tfrac{6}{7}\text{Ti}_5\text{Sn}_3(s) + \text{Sn}(g) \tag{R(4)}$$

The experimental stannides evaporation rates via temperature logarithmic dependence are plotted in Fig. 3. Evaporation rate of stannides is higher than evaporation rate of pure titanium but lower than for pure tin in temperature interval 1566–1834 K. The temperature dependence of total tin vapour (P, Pa) and evaporation rates (G, kg m^{-2} s^{-1}) for reactions calculated by least squares method can be best represented by logarithmic equation $\ln G = -[(A \pm \Delta A)10^{-4} \, T^{-1} - (B \pm \Delta B)]$ and linear regression $\ln P = -[(a \pm \Delta a)10^4 \, T^{-1} - (b \pm \Delta b)]$ which was reported in [8]. The equations empirical coefficients are listed in Table 1.
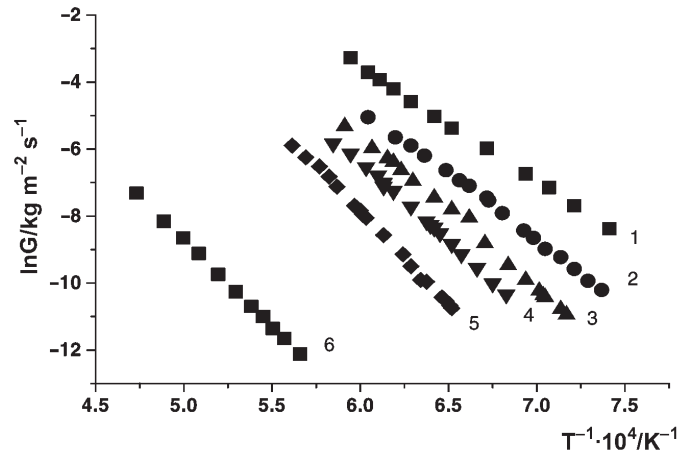
Fig. 3 Experimental $H^o(T)$–H^o(298.15 K) enthalpy dependence *vs.* temperature

Table 1 Empirical coefficients of total tin vapor (P, Pa) and evaporation rates (G, kg m^{-2} s^{-1}) temperature dependency equations

Chemical formula	Temp. range/K	$\ln P= -[(a\pm\Delta a)10^4\ T^{-1}-(b\pm\Delta b)]$		$\ln G= -[(A\pm\Delta A)10^{-4}\ T^{-1}-(B\pm\Delta B)]$	
		$a\pm\Delta a$	$b\pm\Delta b$	$A\pm\Delta A$	$B\pm\Delta B$
Ti$_3$Sn	1565–1835	5.487±0.121	30.826±0.719	5.399±0.119	23.545±0.708
Ti$_2$Sn	1500–1770	4.413±0.154	26.111±0.949	4.335±0.154	18.890±0.951
Ti$_5$Sn$_3$	1440–1735	4.355±0.160	26.435±0.997	4.260±0.160	19.113±0.998
Ti$_6$Sn$_5$	1390–1700	3.954±0.035	25.132±0.227	4.293±0.121	19.243±0.749

Thermodynamic function temperature dependence study

Previously the values of $(H^o_{310} - H^o_{298.15})$ were determined using low temperature regime of calorimeter. The formation enthalpy of titanium stannides found to be 63.13, 55.56, 154.94 and 215.67 kJ mol^{-1} for Ti$_3$Sn, Ti$_2$Sn, Ti$_5$Sn$_3$ and Ti$_6$Sn$_5$, correspondingly. Determined by differential scanning calorimetry enthalpy values are in good agreement with data for other stannides types [9], contrary to [10], which data are ground-less large. Using enthalpy data the heat capacities C_p (298.15 K) were calculated to be 100.23, 72.94, 195.94 and 272.18 J mol^{-1} K^{-1} for Ti$_3$Sn, Ti$_2$Sn, Ti$_5$Sn$_3$ and Ti$_6$Sn$_5$, respectively.

The enthalpy temperature dependence for high temperature region (360–1150 K) is plotted in Fig. 3. Observed monotonous enthalpy increase with temperature rises is in agreement with phase transition absence in chosen temperatures. The experimentally enthalpy data were used for thermodynamic function calculation (1–3).

$$C_p = dH/dT \tag{1}$$

$$\Delta S = \int_{T_1}^{T_2} \frac{C_p}{T} dt \tag{2}$$

$$\Delta G_{298}^{T} = \Delta H_{298}^{T} - T\Delta S_{298}^{T} \tag{3}$$

The enthalpy temperature dependence ($H^\circ(T,K)$–H°(298.15 K)) can be best explained using Maier and Kelly equation [11]:

$$H^\circ(T) - H^\circ(298.15\,K) = AT^2 + BT + CT^{-1} + D \tag{4}$$

Note: A, B, C, D – coefficients.

Thus temperature dependence of specific heat capacity, entropy and Gibbs energy can be calculated according to Eqs (5)–(8):

$$C_P^\circ(T) = 2AT + B - CT^{-2} \tag{5}$$

$$S^\circ(T) - S^\circ(298.15\,K) = 2AT^{2+B} + B\ln T + 0.5CT^{-2} + E \tag{6}$$

$$G'(T) - G'(298.15\,K) = AT + B\ln T - DT^{-1} - 0.5CT^{-2} + [E-B] \tag{7}$$

$$E = -(596.3A + 5.698B + 5.625 \cdot 10^{-6}C) \tag{8}$$

Note: E – coefficient.

Coefficients of Eqs (4)–(8) for thermodynamic function temperature dependence are listed in Table 2.

Table 2 Coefficients of thermodynamical functions Eqs (4)–(8)

Chemical formula	Temperature range/K	A	B	C	D	E
Ti_3Sn	380–1150	617.7	100.630	362 959	–31 769	–579.07
Ti_2Sn	360–1110	101.7	69.207	207 382	–22 234	–401.57
Ti_5Sn_3	375–1110	258.3	191.033	936 493	–62 393	–1156.59
Ti_6Sn_5	410–1110	307.2	261.666	692 137	–83 068	–1548.22

The total tin vapour (P, Pa) pressure *vs.* temperature dependence was used for $\Delta_r H^\circ$(298.15 K) standard enthalpy of reactions (1)–(4) calculation according to thermodynamics second-low treatment, such values were also calculated by Kirchoff equation:

$$\Delta_r H^\circ(298.15\,K) = \Delta_r H^\circ(T_{aver}) - H^\circ(T,K) - H^\circ(298.15\,K) \tag{9}$$

Obtained values lies in short interval listed in Table 3.

Table 3 Standard enthalpy of reactions (1)–(4) and atomization of titanium stannides

Chemical formula	$\Delta_r H^o$(298.15K), kJ mol^{-1}	ΔH^o_{st}(298.15 K)	
		kJ mol^{-1}	kJ g-atom^{-1}
Ti$_3$Sn	364.13±2.5	1760	440.0
Ti$_2$Sn	342.18±1.5	1287	429.0
Ti$_5$Sn$_3$	333.32±1.8	3384	423.0
Ti$_6$Sn$_5$	318.21±1.4	4512	410.2

Atomisation enthalpies of stannides evaporation reactions (1)–(4) have been calculated by additivity. It was established that ΔH^o_{st}(298.15 K) value is increasing from Ti$_3$Sn to Ti$_6$Sn$_5$ by linear order, which is caused by decrease of interatomic interaction with tin content enlarging in stannides.
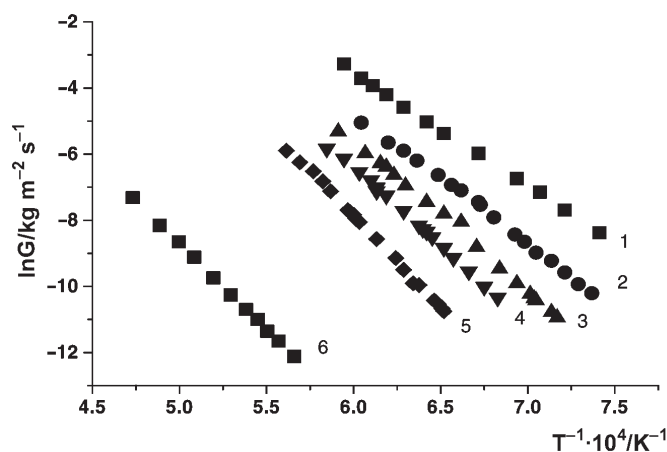

Fig. 4 The logarithmic dependence of evaporation rates via temperature for
1 – Sn; 2 – Ti$_5$Sn$_6$; 3 – Ti$_5$Sn$_3$; 4 – Ti$_2$Sn; 5 – Ti$_3$Sn; 6 – Ti

Conclusions

A method of bulk crystals growth for titanium stannides was elaborated. A series of stannides Ti$_3$Sn, Ti$_2$Sn, Ti$_5$Sn$_3$ and Ti$_6$Sn$_5$ were obtained by crucible-less growth techniques under vacuum. Temperature dependence equations for total tin vapour and evaporation rate have been suggested. The enthalpy, specific heat capacity, entropy and Gibbs energy temperature dependence were simulated using Maier and Kelly equations. Atomisation enthalpy is increasing from Ti$_3$Sn to Ti$_6$Sn$_5$ by linear order with tin content enlarging.

References

1 O. V. Podarevskaya, Ph. D. Thesis, Institute for Foundry Problem, Kiev 1996.
2 O. M. Koval and Yu. N. Barabash, Crystal structure of Metals and Alloys, Naukova Dumka, Kiev 1986.
3 T. B. Massolski, H. Okamoto, P. R. Subramanian and L. Kacprzak (eds.), Binary Alloy Phase Diagrams, ASM International, Materials Park, OH 1990.
4 M. E. Brown, Introduction to Thermal Analysis: Techniques and Applications, Chapman and Hall, London, New York 1988.
5 E. A. Gulbransen and F. A. Brassart, in: Microweighting in vacuum and controlled environments, A. W. Czandera and A. Wolsky (Eds), Elsevier, Amsterdam 1980.
6 D. Stull and B. Prophet, JANAF Thermochemical Tables, National Standard Reference Data System, NSRDS-NBS 37, DC, 2nd ed., Washington 1971.
7 V. V. Fesenko, O. V. Podarevskaya and V. V. Timochin, Device for evaporation rate measurement at high-temperatures, USFT publishers, Kiev 1986.
8 B. A. Kireev, Methods of practical calculation in thermodynamic of chemical reaction, Khimia, 3rd edn., Moscow 1992.
9 Yu. O. Esin, M. G. Valishev, A. F. Ermakov, V. I. Petrov and S. V. Mikhailov, Zh. Fiz. Khimii, 55 (1985) 747.
10 V. D. Savin, Zh. Fiz. Khimii, 47 (1973) 2528.
11 C. G. Maier and K. K. Kelly, J. Amer. Chem. Soc., 54 (1932) 3243.